The gametic central cell of *Arabidopsis* determines the lifespan of adjacent accessory cells

Christina Kägi, Nadine Baumann, Nicola Nielsen, York-Dieter Stierhof, and Rita Groß-Hardt[1]

Center for Plant Molecular Biology, University of Tübingen, 72076 Tübingen, Germany

Edited by Robert L. Fischer, University of California, Berkeley, CA, and approved November 3, 2010 (received for review August 27, 2010)

Plant germ cells develop in specialized haploid structures, termed gametophytes. The female gametophyte patterns of flowering plants are diverse, with often unknown adaptive value. Here we present the *Arabidopsis fiona* mutant, which forms a female gametophyte that is structurally and functionally reminiscent of a phylogenetic distant female gametophyte. The respective changes include a modified reproductive behavior of one of the female germ cells (central cell) and an extended lifespan of three adjacent accessory cells (antipodals). *FIONA* encodes the cysteinyl t-RNA synthetase SYCO ARATH (SYCO), which is expressed and required in the central cell but not in the antipodals, suggesting that antipodal lifespan is controlled by the adjacent gamete. SYCO localizes to the mitochondria, and ultrastructural analysis of mutant central cells revealed that the protein is necessary for mitochondrial cristae integrity. Furthermore, a dominant ATP/ADP translocator caused mitochondrial cristae degeneration and extended antipodal lifespan when expressed in the central cell of wild-type plants. Notably, this construct did not affect antipodal lifespan when expressed in antipodals. Our results thus identify an unexpected noncell autonomous role for mitochondria in the regulation of cellular lifespan and provide a basis for the coordinated development of gametic and nongametic cells.

cell–cell communication | gametes | programmed cell death

In angiosperms, gametes form in few-celled haploid structures, termed gametophytes. The female gametophyte of most flowering plants originates from a single haploid spore through three syncytial division cycles. Subsequent cellularization generates two synergids, three antipodal cells, and two types of female gametes, an egg and a central cell. The different cell types have distinct functions in the reproductive process. Synergids mediate short-range pollen tube attraction and direct the subsequent release of the two sperm cells (1). The fertilized egg gives rise to an embryo, and the fusion of the second sperm cell with the central cell initiates the formation of endosperm, which nurtures the developing embryo. The central cell initially comprises two haploid polar nuclei, which, in many flowering plant species, fuse before fertilization, generating a diploid secondary nucleus (2). The diploid status of the central cell translates into triploid endosperm with a maternal/paternal ratio of 2:1. This ratio has been shown to critically impact on seed size as, for example, a relative decrease in the maternal contribution results in bigger seeds (3). Antipodals, the accessory cells that lie adjacent to the central cell, might also play a nutritive role by transferring nutrients from the maternal sporophyte to the female gametophyte (4). In several grass species, like wheat and maize, antipodal cells proliferate (5). By contrast, in most higher eudicots antipodal cells do not persist but undergo programmed cell death (PCD) (4) (Fig. 1 *A*–*C*). The adaptive value of this derived developmental program (2) is unclear. Recent studies have demonstrated a remarkable developmental plasticity of antipodal cells: in *lachesis* and *clotho* mutants, which are defective for the putative splicing factors PRP4 and Snu114, respectively, antipodals can adopt a central cell fate (6, 7). Furthermore, overexpression of an auxin biosynthesis gene can activate egg cell marker expression in antipodal cells (8). The gametic potential of antipodal cells has raised the hypothesis that antipodal cells act as a backup in case of gametic failure (6). However, to this end it is not known how PCD in antipodal cells is activated or bypassed. In the present work we show that PCD in antipodals is suppressed after mitochondrial dysfunction in the central cell. Our results thus provide a mechanistic basis for the coordinated development of both cell types and reveal a unique noncell autonomous mechanism for the regulation of cellular lifespan.

Results and Discussion

***FIONA* Is Necessary for the Fusion of Central Cell Nuclei.** We have isolated the *fiona* mutant in an ethyl methanesulfonate (EMS)-induced screen for female gametophytic mutants. Heterozygous *fiona* plants exhibit 24.6% infertile seeds (Fig. 1 *D* and *E*; n = 1045), suggesting that homozygous *fiona* mutants are embryo lethal. Light microscopy inspection revealed that the infertile seeds correspond to early embryo and endosperm arrests, revealing an essential role of *FIONA* during seed development (Fig. S1). Because we could not recover homozygous plants, we performed all of the analyses on heterozygous mutants, which segregate 50% wild type and 50% mutant gametophytes. In wild type, the central cell initially comprises two haploid polar nuclei, which mainly fused before fertilization, resulting in the formation of a large secondary nucleus (Fig. 1 *F* and *H*). By contrast, in most *fiona* female gametophytes, polar nuclei size was slightly reduced and the nuclei failed to fuse (Fig. 1 *G* and *H*). Defects in polar nuclei fusion have been reported for several female gametophytic mutants (9–11). In *lachesis* and *clotho* mutants, the fusion defect is a likely consequence of a misspecified central cell (6, 7). To test whether *fiona* central cells were similarly affected, we introduced two central cell markers. Marker expression in *fiona*/*FIONA* was comparable to wild type (Fig. 1 *I*–*L*), suggesting that the central cell identity was not broadly perturbed.

***FIONA* Regulates PCD of Antipodal Cells.** In addition to the alterations in central cell development, we frequently observed persistent antipodal cells in *fiona* mutant gametophytes (Fig. 1 *F*–*H*), indicating that the developmental program that ultimately results in antipodal cell death requires *FIONA* activity. In *lachesis* and *clotho* mutants, defects in antipodal cell death correlate with the progressive conversion of antipodal cells into central cells (6, 7). By contrast, *fiona* antipodals did not seem to switch cell fate, as evidenced by the correct expression of two antipodal cell markers (Fig. 1 *M*–*P*) and a lack of *pMEA::NLS_GUS* central cell marker expression in antipodal cells (n = 499). These results indicated that *FIONA* interferes with a process downstream of antipodal cell commitment but upstream of the PCD pathway. The overall morphology of the egg cell and synergids in *fiona* mutants was normal, and egg cell marker expression was unaltered (Fig. S2 *A*

Author contributions: C.K. and R.G.-H. designed research; C.K., N.B., N.N., and Y.-D.S. performed research; R.G.-H. contributed new reagents/analytic tools; C.K., N.B., N.N., Y.-D.S., and R.G.-H. analyzed data; and C.K. and R.G.-H. wrote the paper.

The authors declare no conflict of interest.

This article is a PNAS Direct Submission.

[1]To whom correspondence should be addressed. E-mail: rita.gross-hardt@zmbp.uni-tuebingen.de.

This article contains supporting information online at www.pnas.org/lookup/suppl/doi:10.1073/pnas.1012795108/-/DCSupplemental.

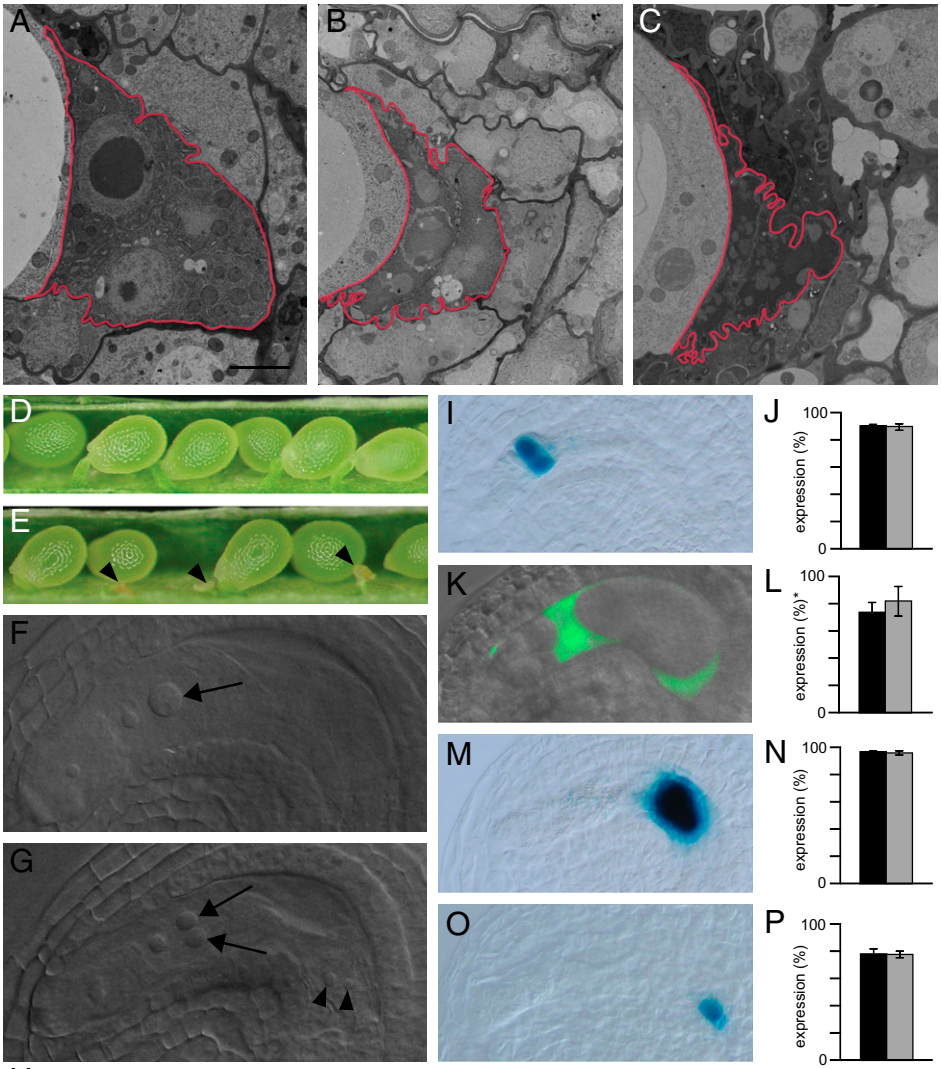

H

Genotype	Polar nuclei unfused (%)	Antipodal nuclei visible (%)	n
FIONA/*FIONA*	4.3	5.5	256
fiona/*FIONA*	30.1	32.2	342

Fig. 1. *fiona* mutants exhibit defects in polar nuclei fusion and an extended antipodal lifespan. (*A*–*C*) Antipodals in wild-type (*A*) 1 d, (*B*) 2 d, and (*C*) 3 d after emasculation. The antipodals are marked by a red border. (Scale bar, 2 μm.) (*D*) Wild-type silique showing full seed set. (*E*) Silique of a selfed *fiona*/*FIONA* plant containing normal and aborted seeds (arrowheads). (*F* and *G*) Whole-mount clearings of gametophytes 2 d after emasculation. (*F*) Wild-type gametophyte containing a secondary nucleus in the central cell (arrow). (*G*) *fiona* gametophyte containing unfused polar nuclei (arrows) and persisting antipodal cells (arrowheads). (*H*) Frequencies of unfused polar nuclei and persistent antipodal cells in wild-type and *fiona*/*FIONA* plants. (*I*–*P*) Expression of central cell and antipodal cell marker genes. Black bars represent wild-type, gray bars represent *fiona*/*FIONA* plants. (*I*) Expression of the central cell marker *pMEA::NLS_GUS* (7). (*J*) Frequencies of ovules expressing *pMEA::NLS_GUS*; n = 534 for wild type, n = 499 for *fiona*/*FIONA*. (*K*) Expression of the central cell marker *DD22::GFP* (35). (*L*) Frequencies of ovules expressing *DD22::GFP*; n = 176 for wild type, n = 151 for *fiona*/*FIONA*. *For ease of comparison the scores from *DD22::GFP*/- plants were adjusted to a homozygous marker situation. (*M*) Expression of the antipodal cell marker *pAt1g36340::GUS* (16). (*N*) Frequencies of ovules expressing *pAt1g36340::GUS*; n = 395 for wild type, n = 549 for *fiona*/*FIONA*. (*O*) Expression of the antipodal cell marker GT3733. (*P*) Frequencies of ovules expressing GT3733; n = 275 for wild type, n = 262 for *fiona*/*FIONA*. Gametophytes were analyzed 2 d after emasculation. Error bars, mean ± SEM.

and *B*). Light-microscopy inspection revealed an occasional increase in synergid nucleolus size (5%, n = 342), and expression of the synergid marker ET2634 (6) was slightly reduced (Fig. S2 *C*–*F*). This phenotype, however, did not affect the pollen tube attracting activity of the synergids (Fig. S2*G*).

Nuclear Fusion in *fiona* Central Cells Relies on Paternal Cues. A common feature of previously described polar nuclei fusion mutants is their reduced fertility (6, 7, 9, 11). Most of these mutants fail to proceed beyond the haploid phase. The recently described *bip1-4 bip2-1* double mutant does get fertilized despite an apparent polar nuclei fusion defect; however, the resulting seeds abort (12). In *bip1-4 bip2-1*, central cell proliferation seems to be initiated prematurely after fusion of the male sperm nucleus to only one of the polar nuclei, resulting in the formation of diploid instead of triploid endosperm.

To our surprise, *fiona* gametophytes were fully fertile when pollinated with wild-type pollen (Fig. 2*A*), and the *fiona* mutation was transmitted through the female without significant decrement (Fig. 2*B*). Importantly, the frequency of unfused polar nuclei in *fiona* female gametophytes remained constant even when the flowers were kept artificially unfertilized over a period of 4 d (n = 140). This contrasts markedly with the situation in, for example, *slow walker1* and *slow walker2* mutants, in which unfused polar nuclei result from a developmental delay of the female gametophyte (13, 14). We therefore reasoned that the fertility of mutant gametophytes was likely to be due to a fertilization-triggered polar nuclei fusion. Alternatively, we could not exclude the possibility that in *fiona*, similar to the situation in *bip1-4 bip2-1* double mutants, diploid endosperm is formed, resulting from fusion of the male sperm nucleus to one of the haploid polar nuclei. The latter scenario would consequently affect the maternal/paternal ratio of the endosperm. We, therefore, measured seed size and determined endosperm ploidy as an indirect readout of polar nuclei fusion. Seeds derived from *fiona*/*FIONA* plants were comparable in size to wild-type seeds (wild type 429 μm, n = 533; *fiona*/*FIONA* 432 μm, n = 484). Furthermore, the endosperm nuclei in *fiona*/*FIONA* seeds were uniform in size and did not differ from wild type (n = 156 for wild type; n = 154 for *fiona*/*FIONA*), which contrasts with the situation in *bip1-4 bip2-1* double mutants, which exhibit irregular nuclei size in the endosperm (12).

Additionally, flow cytometry analysis of *fiona*/*FIONA* seeds detected a 3C peak, as in wild type (Fig. 2 *C* and *D*). This profile contrasted with the one generated for *fie*/*FIE* mutants (Fig. 2*E*),

A

Parental genotype		Seed phenotype in %			
female	male	fertile	aborted	unfertilized	n
fiona/FIONA	*fiona*/FIONA	75.4	19.8	4.8	1,045
FIONA/FIONA	FIONA/FIONA	93.9	2.4	3.7	708
fiona/FIONA	FIONA/FIONA	92.3	1.8	5.9	920

B

Parental genotype		Progeny genotype		
female	male	*fiona*/FIONA	FIONA/FIONA	TE
fiona/FIONA	FIONA/FIONA	187	197	94,9%
FIONA/FIONA	*fiona*/FIONA	142	196	72,4%

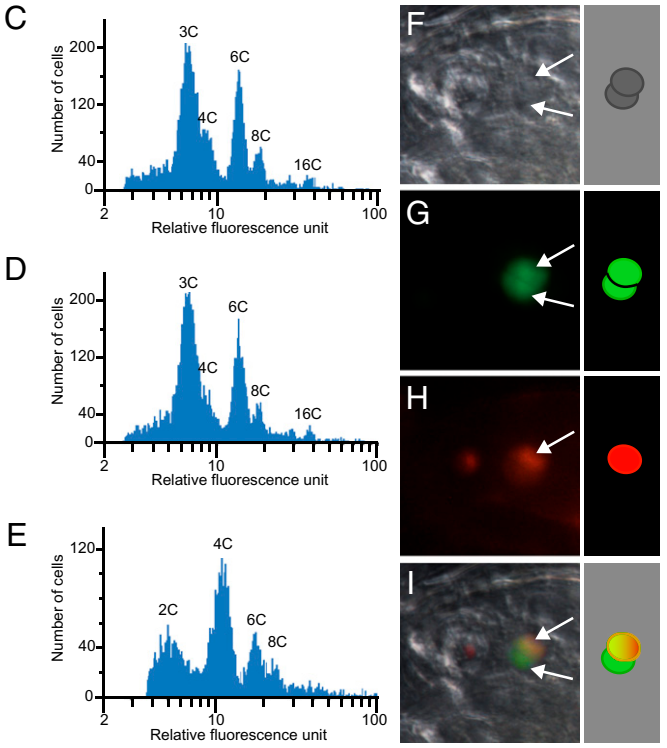

Fig. 2. *fiona* mutant female gametophytes give rise to viable seeds. (*A*) Analysis of siliques resulting from crosses of *fiona*/FIONA and FIONA/FIONA plants. (*B*) Segregation analysis of *fiona,* as determined by reciprocal crosses between *fiona*/FIONA and FIONA/FIONA plants and PCR-based genotyping of the progeny. TE, transmission efficiency. (*C*) Flow cytometry ploidy analysis of seeds derived from wild-type plants. (*D*) Flow cytometry ploidy analysis of seeds derived from *fiona*/FIONA plants. (*E*) Flow cytometry ploidy analysis of seeds derived from emasculated *fie*/FIE flowers. (*F–I*) Fertilization of a *fiona* mutant gametophyte expressing *pAt5g40260::NLS_GFP* with sperm cells expressing *HTR10-mRFP1*. Arrows point at the polar nuclei. (*F*) Bright-field image. (*G*) pAT5g40260::NLS_GFP. (*H*) HTR10-mRFP1. (*I*) Overlay.

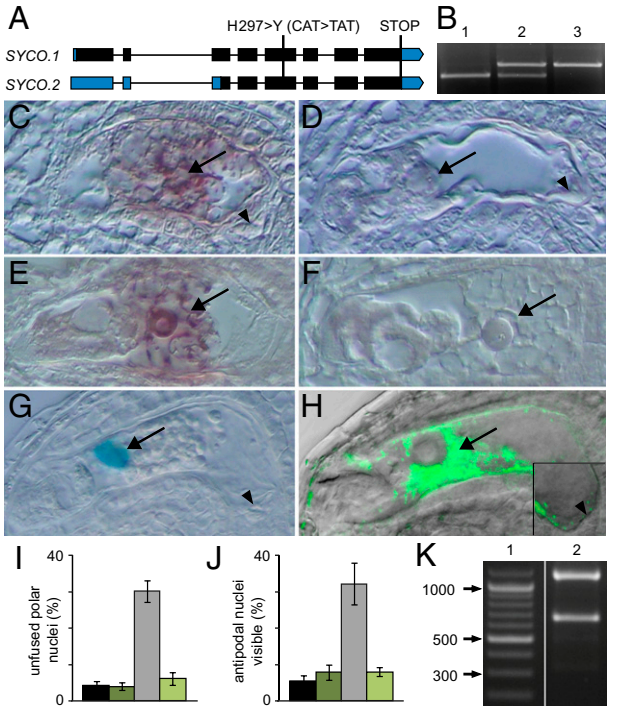

Fig. 3. The cysteinyl-tRNA synthetase *SYCO* is expressed and required in the central cell but not in antipodals. (*A*) Gene structure of *SYCO*. Exons are depicted in bars, introns in lines. UTRs are indicated in blue, coding exons in black. The change in DNA and amino acid sequence in *syco-1* is indicated. (*B*) PCR-based genotyping of the *SYCO* locus reveals that the genomic *SYCO* DNA driven by a 1.25-kb upstream promoter allows the generation of homozygous mutants. 1, *SYCO/SYCO*; 2, *syco-1/SYCO*; 3, *syco-1/syco-1*, *pSYCO::SYCO/-*. (*C–F*), In situ hybridization of *SYCO* mRNA in the female gametophyte before (*C* and *D*) and after (*E* and *F*) antipodal degeneration. (*C* and *E*) Antisense probe. (*D* and *F*) Sense probe. Arrow and arrowhead point at central cell and antipodals, respectively. (*G*) *NLS_GUS* expression driven by a 1.25-kb promoter fragment upstream of *SYCO* is restricted to the central cell nucleus (arrow). (*H*) Localization of pMEA::SYCO_GFP in the central cell (arrow) of the female gametophyte 2 d after emasculation (overlay of GFP fluorescence with differential interference contrast image). *Inset:* Magnification of the proximal end of the central cell and of the antipodals (arrowhead). (*I* and *J*) *pMEA::SYCO_GFP* complements the polar nuclei fusion (*I*) and antipodal PCD (*J*) defects in *syco-1/SYCO* plants. Black bar, wild type, n = 256; dark green bar, *pMEA::SYCO_GFP*, n = 355; gray bar, *syco-1/SYCO*, n = 342; light green bar, *syco-1/SYCO, pMEA::SYCO_GFP*, n = 426. Gametophytes were analyzed 2 d after emasculation. Error bars, mean ± SEM. (*K*) Digestion of PCR-amplified *SYCO_GFP* with BspMI discriminates between *SYCO.1* and *SYCO.2* cDNA. *SYCO.1* is digested to 1,162 bp and 666 bp, *SYCO.2* to 1,162 bp, 338 bp, and 332 bp. 1, ladder; 2, *pMEA::SYCO_GFP*.

which form autonomous diploid endosperm in the absence of fertilization (15). To trace the fusion of male and female gametes during fertilization in *fiona* gametophytes, we generated *fiona*/*FIONA* plants expressing a nuclear-localized GFP under control of the gametophyte specific promoter *pAt5g40260* (16). We then pollinated *fiona*/*FIONA, pAt5g40260::NLS_GFP* plants with pollen expressing the sperm cell-specific reporter gene *HTR10-mRFP1* (17). In *fiona* gametophytes, we observed unfused polar nuclei, of which one had fused with a sperm nucleus (Fig. 2 *F–I*), confirming that central cell nuclei in *fiona* can undergo karyogamy (n = 9).

Intriguingly, the female gametophyte of *fiona* mutants shares morphological and mechanistic similarities with the female gametophyte of several grass species, such as wheat. In wheat, nuclei fusion in the central cell is initiated after fertilization by heterotypic fusion between the male sperm nucleus and one of the polar nuclei (18). Furthermore, antipodal cells do not undergo PCD but persist. In view of the similarities between the fully fertile *fiona* gametophytes and the gametophyte pattern of wheat, it is tempting to speculate whether a FIONA-related mechanism has been used during evolution, accounting for part of the diversity found among flowering plant female gametophytes.

The Gametic Central Cell Triggers PCD of Adjacent Antipodal Cells. We mapped the *fiona* mutation to the At2g31170 locus, which codes for SYCO ARATH, one of three cysteinyl-tRNA synthetases encoded by the *Arabidopsis* genome (19). In the following we will refer to the gene as *SYCO* and to *fiona* as *syco-1*. In *syco-1*, a single base pair mutation causes an amino acid exchange from histidine to tyrosine on position 297 of a total of 563 amino acids (Fig. 3*A*). This histidine is one of five conserved histidine residues at the base of the catalytic center and is important for protein function in *Escherichia coli* (20). Expression of *SYCO* genomic DNA, driven by a 1.25-kb upstream promoter fragment, was able to rescue the mutant phenotype, suggesting that *syco-1* is a loss-of-

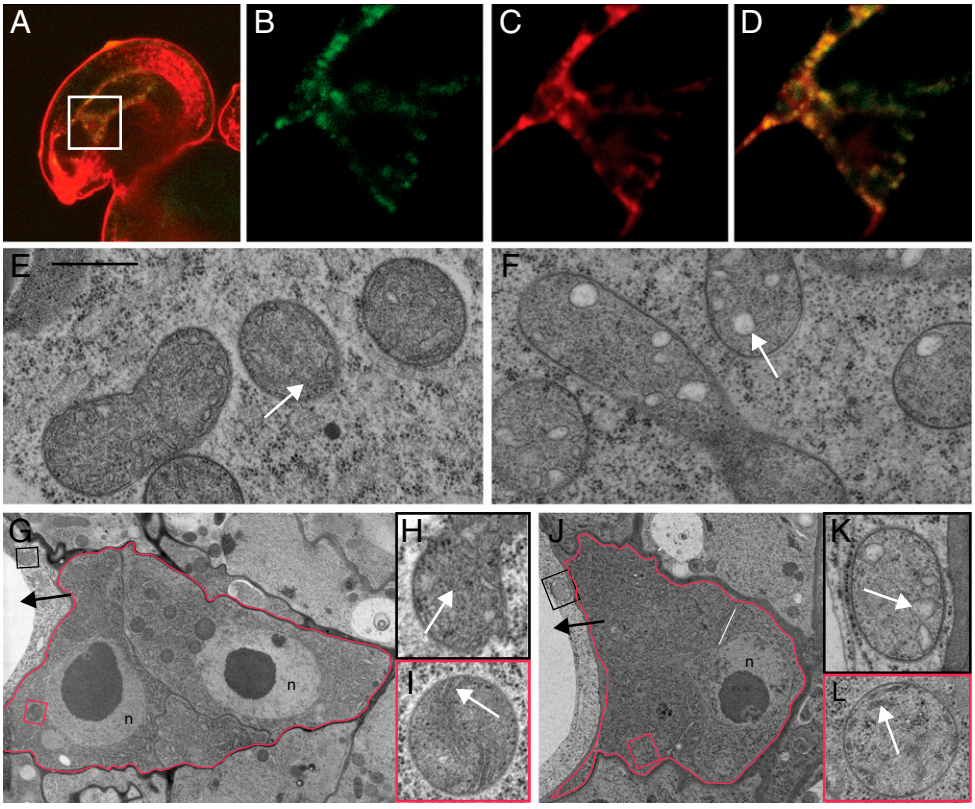

Fig. 4. SYCO localizes to mitochondria and is necessary for cristae integrity in the central cell. (*A–D*) Subcellular localization of SYCO_GFP in the central cell. (*A*) Entire ovule (overlay). (*B–D*) Magnification of box in *A*. (*B*) pMEA:: SYCO_GFP. (*C*) MitoTrackerOrange. (*D*) Overlay. (*E* and *F*) Mitochondria of wild-type (*E*) and *syco-1* (*F*) central cells 2 d after emasculation. (*G*) Antipodal cells (red border) of a wild-type gametophyte 0 d after emasculation. (*H* and *I*) Magnification of boxes in *G*: central cell mitochondrium (*H*) and antipodal mitochondrium (*I*). (*J*) Antipodal cells (red border) of a *syco-1* gametophyte 2 d after emasculation. (*K* and *L*) Magnification of boxes in *J*: central cell mitochondrium (*K*) and antipodal cell mitochondria (*L*). Black arrow, central cell; white arrow, cristae; n, nucleus. (Scale bar, 500 nm in *E*, *F*, *H*, *I*, *K*, and *L*.)

function mutation (Fig. 3*B*). RT-PCR detected *SYCO* expression throughout the plant (Fig. S3*A*). To determine the temporal and spatial expression pattern of *SYCO* in the female gametophyte, we generated promoter reporter constructs and determined *SYCO* mRNA distribution using in situ hybridization. In mature female gametophytes, a clear hybridization signal was found in the central cell (Fig. 3 *C–F*). In agreement with this, *GUS* expression in the female gametophyte of *pSYCO::NLS_GUS* plants was exclusively detected in the central cell (Fig. 3*G*). We did not detect any *pSYCO::NLS_GUS* expression before cellularization (Fig. S3 *B* and *C*; $n = 250$). These results suggest that the extended lifespan of *syco-1* antipodal cells is an indirect consequence of the modified developmental program of the central cell. To test whether central cell expression of *SYCO* was sufficient to complement the mutant defects, we expressed a *SYCO_GFP* fusion protein under the control of the central cell specific *MEDEA* (*MEA*) promoter (Fig. 3*H*), which did not confer expression before cellularization in *syco-1*/*SYCO pMEA::SYCO_GFP* plants ($n = 115$).

As expected, expression of *pMEA::SYCO_GFP* in a *syco-1* mutant background reconstituted the original central cell program, resulting in polar nuclei fusion (Fig. 3*I*). Importantly, PCD of antipodals was also restored to wild-type levels (Fig. 3*J*), indicating that antipodal cell death is triggered by the central cell. The competence of the antipodals to adopt a gametic cell fate has led to the hypothesis that antipodals might serve as a backup for the central cells (6). Our results imply that central cell integrity is a critical parameter determining antipodal lifespan, which is in agreement with this theory.

Mitochondrial Dysfunction in the Central Cell Extends Antipodal Lifespan. *SYCO* possesses two splice variants (Fig. 3*A*). In contrast to SYCO.2, SYCO.1 contains a unique N-terminal domain, which, in transient expression studies, was shown to target GFP to the mitochondria and chloroplasts (21). To determine which splice variant is generated in the female gametophyte, we amplified cDNA from plants expressing *SYCO_GFP* in the central cell, using primers that discriminated against endogenous *SYCO* cDNA. By this means, we mainly detected *SYCO.1*, indicating that the predominant variant generated in the central cell contains the dual targeting sequence (Fig. 3*K*). To determine the subcellular localization of SYCO *in planta*, we analyzed the GFP-tagged version of the protein in the central cell. pMEA:: SYCO_GFP accumulated in patches and colocalized with the mitochondrion-specific dye MitoTracker Orange (Fig. 4 *A–D*).

The subcellular SYCO distribution prompted us to investigate the mitochondria in the central cell and antipodal cells of *syco-1* gametophytes. Ultrastructural analysis on sections of wild-type gametophytes detected mitochondria containing numerous clearly visible cristae (Fig. 4 *E* and *G–I*). Corresponding sections of *syco-1* gametophytes revealed a regular morphology in the mitochondria of antipodal cells (Fig. 4 *J* and *L*). By contrast, the mitochondria of the central cell lacked regular cristae (Fig. 4 *F* and *K* and Fig. S4), indicating that SYCO is necessary for the integrity of central cell mitochondria.

To determine whether there is a causal relationship between the integrity of central cell mitochondria and the lifespan of antipodals, we aimed to specifically impair the mitochondrial function in the central cells of wild-type plants. The mitochondrial ATP/ADP translocator AAC is a key enzyme in the inner membrane of mitochondria, and the ADP/ATP catalyzing function of AAC2 is conserved between yeast and plants (22). In yeast, a dominant mutation is described which impairs the electron transport chain, resulting in membrane uncoupling (23). We introduced an analogous mutation into *Arabidopsis* AAC2 (Fig. S5) and expressed this dominant version from a central cell promoter. As expected, *pMEA::aac2*^{A199D}*_GFP* hemizygous plants segregated 50% gametophytes which expressed the construct specifically in the central cell (Fig. 5*A*). Ultrastructural analysis revealed that the respective central cell mitochondria lack regular cristae (Fig. 5 *B* and *C*), confirming the conserved role of AAC2 for mitochondrial mem-

brane integrity. We next analyzed the morphology of *pMEA::aac2^{A199D}_GFP* plants by performing cleared whole mounts. In two independent transgenic lines we observed unfused polar nuclei (Fig. 5 *D*, *F*, and *G*), indicating that nuclei fusion in the central cell is indeed a mitochondria-dependent process. Importantly, this construct additionally repressed PCD of antipodals (Fig. 5 *E*–*G*). By contrast, expression of *aac2^{A199D}* in antipodals, making use of the promoter *pHSFa2* (Fig. 5*H*), did not significantly affect antipodal PCD, as evidenced by the analysis of independent transgenic lines (Fig. 5 *I* and *J*). Our data thus establish an essential role of central cell mitochondria for antipodal PCD.

Conclusions

Mitochondria are the principal energy source of the cells. In plants, they have also been implicated in polar nuclei fusion, which is prohibited after mutations in the mitochondrial ribosomal subunit L21 (11) or a mitochondria-localized DnaJ protein (9). Here we have shown that cristae degeneration induced by expression of the dominant *aac2^{A199D}* allele prevents polar nuclei fusion, confirming the proposed role of mitochondria during nuclear fusion (11) (Fig. 5*K*). Mitochondria have, in addition, long been recognized to be associated with PCD in both plants and animals (24, 25), and their dysfunction has been shown to correlate with cell and organismal aging in yeast, invertebrates, and mammals (26). Seemingly paradox, the reduction of mitochondria function can also extend lifespan as shown for *Caenorhabditis elegans* and *Drosophila* (27, 28). The mechanisms that underlie lifespan extension are elusive; however, one theory is that reactive oxygen species, which accumulate as a byproduct of a functional electron transport chain, enhance aging through their damaging effects on mitochondrial DNA (26). Our results suggest that the function of mitochondria in lifespan regulation is conserved in plants. However, the spatial discrepancy between the mitochondrial defect in the central cell and the PCD defect in antipodals is surprising and reveals that mitochondria dysfunction can affect cellular lifespan in a noncell autonomous manner (Fig. 5*K*). The data presented here extend the current view of mitochondria-associated lifespan regulation and draw the attention away from the dying cell and toward adjacent nondying cells as a potential cause for PCD.

syco-1 provides a fascinating example of how small-scale molecular changes can affect complex reproductive traits. The similarity between the female gametophytes of *syco-1* and grasses, together with our finding that *SYCO* is required for mitochondrial cristae integrity, might suggest that differences in the metabolic profile between *Arabidopsis* and wheat central cells account for the distinct female gametophyte patterns of these phylogenetic distant plant species. This theory will remain a topic for future investigation.

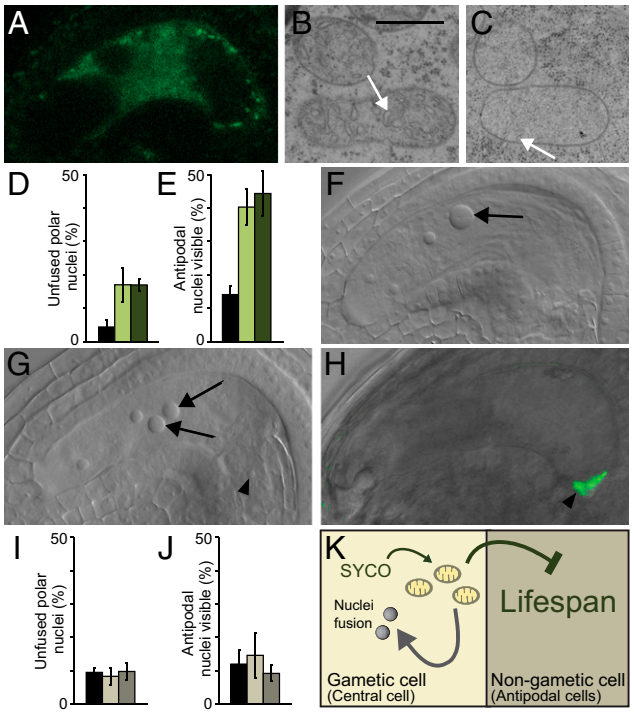

Fig. 5. *aac2^{A199D}* causes mitochondrial cristae degradation and extends antipodal lifespan when expressed in the central cell of wild-type plants. (*A*) Localization of pMEA::aac2^{A199D}_GFP in the central cell of the female gametophyte. (*B* and *C*) Central cell mitochondria in wild type (*B*) and *pMEA::aac2^{A199D}_GFP* (*C*). White arrows indicate cristae. (*D* and *E*) Frequencies of unfused polar nuclei (*D*) and persistent antipodal cells (*E*) in wild-type (black bar) and two independent *pMEA::aac2^{A199D}_GFP* transgenic lines (green bars); n = 361 for wild type, n = 452 for line 1 (*pMEA::aac2^{A199D}_GFP/-*; light green), n = 212 for line 2 (*pMEA::aac2^{A199D}_GFP/pMEA::aac2^{A199D}_GFP*; dark green). Gametophytes were analyzed 2 d after emasculation. (*F* and *G*) Whole-mount clearing of a wild-type (*F*) and *pMEA::aac2^{A199D}_GFP* (*G*) gametophyte 2 d after emasculation. Arrows indicate the fused secondary nucleus and the unfused polar nuclei, respectively. Arrowheads indicate antipodals. (*H*) Localization of *pHSFa2::aac2^{A199D}_GFP* in antipodals (arrowhead) of the female gametophyte (overlay of GFP fluorescence with differential interference contrast image). (*I* and *J*) Frequencies of unfused polar nuclei (*I*) and persistent antipodal cells (*J*) in wild-type (black bar) and two independent *pHSFa2::aac2^{A199D}_GFP/pHSFa2::aac2^{A199D}_GFP* transgenic lines (gray bars); n = 241 for wild type, n = 239 for line 1 (light gray), n = 173 for line 2 (dark gray). (*K*) Model for SYCO function. SYCO-dependent mitochondria integrity is necessary for nuclei fusion in the central cell and negatively regulates antipodal lifespan in a noncell autonomous manner. Error bars, mean ± SEM. (Scale bar, 500 nm in *B* and *C*.)

Materials and Methods

Plant Material and Growth Conditions. Plants were grown on soil in growth chambers under long-day conditions (16 h light/8 h dark) at 20 °C. The *syco-1* allele was isolated from plants containing markers ET1119 and GT3733 (6) in the Landsberg *erecta* (L*er*) accession after mutagenesis; seeds were mutagenized by incubation in 0.15% EMS for 10 h.

Molecular Cloning and Complementation. Mapping of *syco-1* was performed as described previously (29) using polymorphisms annotated by CEREON (30). The Columbia accession (Col-0) was used as the crossing partner. *syco-1* was located to chromosome 2 in an area of 20 kb between polymorphisms CER442808 and CER442815 on BAC T16B12/F16D14. We sequenced all ORFs in this interval and identified a single heterozygous locus in At2g31170.

To generate the *pSYCO::SYCO* complementation construct, a 1,253-bp promoter fragment upstream of the start codon was PCR-amplified from genomic DNA using primers 5′-AGTGAGGCGCGCCTTTTGATTTTGATTTTGTGTTGTTTTTGTCGTTAAGAC-3′ and 5′-AGTGATGATCATGGTGTGGAACGATAAGCTCCTTC-3′. The annotated *SYCO* ORF was amplified from L*er* genomic DNA using primers 5′-AGTGATTAATTAAACTAGTATGGCTTCTTCTGTCCTTAATCTCTTC-3′ and 5′-GAAAAATTATTACGTATCTCATACC-3′. For the translational fusion construct, genomic *SYCO* was amplified using 5′-ACTGACAATTGAGGTGTAGTAGTTACAGGTTCTTG-3′ as antisense primer, released PacI/MfeI and cloned in front of an eGFP lacking the start codon. *AAC2* was amplified from L*er* cDNA using the primers 5′-GTTAATTAATGGTTGAACAGACTCAGCACC-3′ and 5′-ACAATTGGGCACCTCCAGATCCATACTTC-3′. The point mutation A199D was inserted by site-directed mutagenesis (31) using the primer 5′-P-AGGCACCAtCAGCACCTC-3′. The mutated *aac2^{A199D}* was cloned PacI/MfeI in front of an eGFP lacking the start codon. To generate the *pSYCO::NLS_GUS* construct, the same promoter fragment as used for complementation was cloned into binary vector *pGIIBar-pLIS::NLS_GUS* in place of the *LIS* promoter (6). For amplification of the previously published *MEA* promoter (6) primers 5′-AGTGAGGCGCGCCAATAGGTCGAGAAAATGCTGTGAATCG-3′ and 5′-AGTGACGATCGTAACCACTCGCCTCTTCTTTTTTTCTC-3′ were used. For amplification of *pAT5g40260* (16), primers 5′-AGTGAGGCGCGCCTTTCTGTACTTTTGAAAATA-3′ and 5′-AGTGATTAATTAATAAAATCGCCGTTTACAAA-3′ were used.

PCR-based Genotyping. Plants were genotyped for the *syco-1* allele using primers 5′-CCAATTCAGATTCTTGATAATGGC-3′ and 5′-AAGTCTCAGAGCAAGA-

GGATG-3′. The resulting 661-bp fragment was digested with HphI, yielding two fragments of 133 bp and 528 bp from the product of the *syco-1* allele and three fragments of 133 bp, 260 bp, and 268 bp from the product of the wild-type allele. To discriminate against the transgene in plants containing *pSYCO::SYCO* or *pMEA::SYCO_GFP*, primers 5′-CATTGAATACTTGTTTACTCATTTAAGTC-3′ and 5′-ATCACTAACAAAGTATAACCATTAAGC-3′ were used. The resulting 2,248-bp fragment was digested with HphI, yielding 192-bp and 2,056-bp fragments in wild type.

Reverse Transcription–Polymerase Chain Reaction. RNA isolation, reverse transcription, and RT-PCR were performed as previously described (6). *SYCO* cDNA was amplified using primers 5′-AATGGTTTTGTTACTGTTGACTCC-3′ and 5′-AAGTCTCAGAGCAAGAGGATG-3′. To discriminate between the two splice variants in female gametophytes, cDNA from gynoecia (2 d after emasculation) of *pMEA::SYCO_GFP* plants was amplified using primers 5′-CTTCTTCTGTCCTTAATCTCTTC-3′ and 5′-AACTTCAGGGTCAGCTTGC-3′ and digested with BspMI.

Flow Cytometry. For flow cytometry analysis, seeds containing heart-stage embryos were crushed in a 2-mL test tube with nuclear extraction buffer (CyStain UV-precise kit; Partec) using a pistil. For analysis of autonomous endosperm formation in *fie*, seeds from emasculated flowers were harvested. The cells were filtered through a 50-μm CellTrics Filter (Partec) and stained with nuclear staining buffer (CyStain UV-precise kit). Flow cytometry was performed on a Partec Ploidy Analyzer (32). Extraction from young leaves was taken as a reference value.

Histology and Microscopy. For analysis of mature gametophytes, the oldest closed flower bud of a given inflorescence was emasculated and harvested 2 or 4 d later. For counting endosperm nuclei in *syco-1/SYCO* and wild type, whole-mount clearings of 3-d-old crosses with wild-type pollen were analyzed. Cytochemical staining for GUS activity and whole-mount clearings were performed as described previously (6). The GFP constructs and MitoTracker Orange (Molecular Probes) were observed using a Leica TCS-SP2 confocal scanning microscope. Confocal images were obtained with a 63× water-immersion objective lens and via Leica Confocal software. For analysis of the nuclear fusion event, emasculated flowers were pollinated with HTR10-mRFP1 (17) and analyzed under a Leica DMI6000B 10–14 h after pollination.

In situ hybridization on emasculated flowers was performed as described previously (33). The antisense riboprobe was amplified using primers 5′-CTTCTTCTGTCCTTAATCTCTTC-3′ and 5′-TAAGCTTTAATACGACTCACTATAGGGAGACTCAAGAGTACATCGAAAGTGAC-3′, the sense probe was amplified using primers 5′-TAAGCTTTAATACGACTCACTATAGGGAGACTTCTTCTGTCCTTAATCTCTTC-3′ and 5′-CTCAAGAGTACATCGAAAGTGAC-3′.

Ultrastructural analysis of high-pressure frozen, freeze-substituted, and resin-embedded ovules was carried out as previously described (34).

Statistical Analysis. Mutant transmission efficiency was analyzed using a χ^2 test.

ACKNOWLEDGMENTS. We thank F. Berger (Temasek LifeSciences Laboratory, National University of Singapore, Singapore), G. N. Drews (Department of Biology, University of Utah, Salt Lake City), R. Fischer (Plant and Microbial Biology Department, University of California, Berkeley, CA), U. Grossniklaus (Institute of Plant Biology and Zürich Basel Plant Science Center, University of Zürich, Zürich, Switzerland), and V. Sundaresan (Department of Plant Biology, University of California, Davis, CA) for seeds; D. Ripper for technical support; M. Nowack and A. Schnittger for help with ploidy analysis; and F. de Courcy, W. Friedman, P. Kahle, T. Laux, D. Weijers, and members of the R.G.-H. laboratory for helpful discussions and comments on the manuscript. This work was supported by the University of Tübingen, Deutsche Forschungsgemeinschaft Grant SFB446 (to R.G.-H.), and a stipend from the Landesgraduiertenförderung Baden-Württemberg (to C.K.).

1. Dresselhaus T, Márton ML (2009) Micropylar pollen tube guidance and burst: Adapted from defense mechanisms? *Curr Opin Plant Biol* 12:773–780.
2. Williams JH, Friedman WE (2004) The four-celled female gametophyte of Illicium (Illiciaceae; Austrobaileyales): Implications for understanding the origin and early evolution of monocots, eumagnoliids, and eudicots. *Am J Bot* 91:332–351.
3. Scott RJ, Spielman M, Bailey J, Dickinson HG (1998) Parent-of-origin effects on seed development in *Arabidopsis thaliana*. *Development* 125:3329–3341.
4. Holloway SJ, Friedman WE (2008) Embryological features of *Tofieldia glutinosa* and their bearing on the early diversification of monocotyledonous plants. *Ann Bot (Lond)* 102:167–182.
5. Raghavan V (1997) *Molecular Embryology of Flowering Plants* (Cambridge Univ Press, Cambridge, UK).
6. Gross-Hardt R, et al. (2007) LACHESIS restricts gametic cell fate in the female gametophyte of Arabidopsis. *PLoS Biol* 5:e47.
7. Moll C, et al. (2008) CLO/GFA1 and ATO are novel regulators of gametic cell fate in plants. *Plant J* 56:913–921.
8. Pagnussat GC, Alandete-Saez M, Bowman JL, Sundaresan V (2009) Auxin-dependent patterning and gamete specification in the *Arabidopsis* female gametophyte. *Science* 324:1684–1689.
9. Christensen CA, et al. (2002) Mitochondrial GFA2 is required for synergid cell death in *Arabidopsis*. *Plant Cell* 14:2215–2232.
10. Pagnussat GC, et al. (2005) Genetic and molecular identification of genes required for female gametophyte development and function in *Arabidopsis*. *Development* 132:603–614.
11. Portereiko MF, et al. (2006) NUCLEAR FUSION DEFECTIVE1 encodes the Arabidopsis RPL21M protein and is required for karyogamy during female gametophyte development and fertilization. *Plant Physiol* 141:957–965.
12. Maruyama D, Endo T, Nishikawa S (2010) BiP-mediated polar nuclei fusion is essential for the regulation of endosperm nuclei proliferation in *Arabidopsis thaliana*. *Proc Natl Acad Sci USA* 107:1684–1689.
13. Li N, et al. (2009) SLOW WALKER2, a NOC1/MAK21 homologue, is essential for coordinated cell cycle progression during female gametophyte development in *Arabidopsis*. *Plant Physiol* 151:1486–1497.
14. Shi DQ, et al. (2005) SLOW WALKER1, essential for gametogenesis in *Arabidopsis*, encodes a WD40 protein involved in 18S ribosomal RNA biogenesis. *Plant Cell* 17:2340–2354.
15. Ohad N, et al. (1996) A mutation that allows endosperm development without fertilization. *Proc Natl Acad Sci USA* 93:5319–5324.
16. Yu HJ, Hogan P, Sundaresan V (2005) Analysis of the female gametophyte transcriptome of *Arabidopsis* by comparative expression profiling. *Plant Physiol* 139:1853–1869.
17. Ingouff M, Hamamura Y, Gourgues M, Higashiyama T, Berger F (2007) Distinct dynamics of HISTONE3 variants between the two fertilization products in plants. *Curr Biol* 17:1032–1037.
18. Hoshikawa K (1959) Cytological studies of double fertilization in wheat (*Triticum aestivum L.*). *Proc Crop Sci Soc Jpn* 28:142–146.
19. Duchêne AM, et al. (2005) Dual targeting is the rule for organellar aminoacyl-tRNA synthetases in *Arabidopsis thaliana*. *Proc Natl Acad Sci USA* 102:16484–16489.
20. Zhang CM, Perona JJ, Hou YM (2003) Amino acid discrimination by a highly differentiated metal center of an aminoacyl-tRNA synthetase. *Biochemistry* 42:10931–10937.
21. Peeters NM, et al. (2000) Duplication and quadruplication of *Arabidopsis thaliana* cysteinyl- and asparaginyl-tRNA synthetase genes of organellar origin. *J Mol Evol* 50:413–423.
22. Haferkamp I, Hackstein JH, Voncken FG, Schmit G, Tjaden J (2002) Functional integration of mitochondrial and hydrogenosomal ADP/ATP carriers in the *Escherichia coli* membrane reveals different biochemical characteristics for plants, mammals and anaerobic chytrids. *Eur J Biochem* 269:3172–3181.
23. Wang X, Salinas K, Zuo X, Kucejova B, Chen XJ (2008) Dominant membrane uncoupling by mutant adenine nucleotide translocase in mitochondrial diseases. *Hum Mol Genet* 17:4036–4044.
24. Green DR, Reed JC (1998) Mitochondria and apoptosis. *Science* 281:1309–1312.
25. Reape TJ, McCabe PF (2008) Apoptotic-like programmed cell death in plants. *New Phytol* 180:13–26.
26. Bishop NA, Lu T, Yankner BA (2010) Neural mechanisms of ageing and cognitive decline. *Nature* 464:529–535.
27. Copeland JM, et al. (2009) Extension of *Drosophila* life span by RNAi of the mitochondrial respiratory chain. *Curr Biol* 19:1591–1598.
28. Lee SS, et al. (2003) A systematic RNAi screen identifies a critical role for mitochondria in *C. elegans* longevity. *Nat Genet* 33:40–48.
29. Lukowitz W, Gillmor CS, Scheible WR (2000) Positional cloning in *Arabidopsis*. Why it feels good to have a genome initiative working for you. *Plant Physiol* 123:795–805.
30. Jander G, et al. (2002) *Arabidopsis* map-based cloning in the post-genome era. *Plant Physiol* 129:440–450.
31. Sawano A, Miyawaki A (2000) Directed evolution of green fluorescent protein by a new versatile PCR strategy for site-directed and semi-random mutagenesis. *Nucleic Acids Res* 28:E78.
32. Nowack MK, et al. (2007) Bypassing genomic imprinting allows seed development. *Nature* 447:312–315.
33. Mayer KF, et al. (1998) Role of WUSCHEL in regulating stem cell fate in the *Arabidopsis* shoot meristem. *Cell* 95:805–815.
34. Dettmer J, Hong-Hermesdorf A, Stierhof YD, Schumacher K (2006) Vacuolar H +-ATPase activity is required for endocytic and secretory trafficking in *Arabidopsis*. *Plant Cell* 18:715–730.
35. Steffen JG, Kang IH, Macfarlane J, Drews GN (2007) Identification of genes expressed in the *Arabidopsis* female gametophyte. *Plant J* 51:281–292.